Cell Metabolism
Article

PGRN is a Key Adipokine Mediating High Fat Diet-Induced Insulin Resistance and Obesity through IL-6 in Adipose Tissue

Toshiya Matsubara,[1,3,6,10] Ayako Mita,[1,2,10] Kohtaro Minami,[1] Tetsuya Hosooka,[2] Sohei Kitazawa,[4,11] Kenichi Takahashi,[9] Yoshikazu Tamori,[2,7] Norihide Yokoi,[1] Makoto Watanabe,[6,8] Ei-ichi Matsuo,[6,8] Osamu Nishimura,[3,8,*] and Susumu Seino[1,2,3,5,*]

[1]Division of Cellular and Molecular Medicine
[2]Division of Diabetes and Endocrinology
[3]The Integrated Center for Mass Spectrometry
[4]Division of Diagnostic Molecular Pathology
Kobe University Graduate School of Medicine, 7-5-1 Kusunoki-cho, Chuo-ku, Kobe, Hyogo 650-0017, Japan
[5]Core Research for Evolutional Science and Technology (CREST), Japan Science and Technology Agency, 4-1-8 Hon-cho, Kawaguchi, Saitama 332-0012, Japan
[6]Life Science Research Center, Technology Research Laboratory, Shimadzu Corporation, 3-9-4 Hikaridai, Seika-cho, Soraku-gun, Kyoto 619-0237, Japan
[7]Department of Internal Medicine, Diabetes Center, Chibune Hospital, 2-2-45 Tsukuda, Nishiyodogawa-ku, Osaka 555-0001, Japan
[8]Division of Disease Proteomics, Institute for Protein Research, Osaka University, 3-2 Yamadaoka, Suita, Osaka 565-0871, Japan
[9]JCR Pharmaceuticals Co., Ltd., 2-2-10 Murotani, Nishi-ku, Kobe, Hyogo, 651-2241, Japan
[10]These authors contributed equally to this work
[11]Present address: Division of Molecular Pathology, Ehime University School of Medicine, Shitsukawa, Toon, Ehime 791-0295, Japan
*Correspondence: seino@med.kobe-u.ac.jp (S.S.), osamu_nishimura@protein.osaka-u.ac.jp (O.N.)
DOI 10.1016/j.cmet.2011.12.002

SUMMARY

Adipose tissue secretes adipokines that mediate insulin resistance, a characteristic feature of obesity and type 2 diabetes. By differential proteome analysis of cellular models of insulin resistance, we identified progranulin (PGRN) as an adipokine induced by TNF-α and dexamethasone. PGRN in blood and adipose tissues was markedly increased in obese mouse models and was normalized with treatment of pioglitazone, an insulin-sensitizing agent. Ablation of PGRN (*Grn*$^{-/-}$) prevented mice from high fat diet (HFD)-induced insulin resistance, adipocyte hypertrophy, and obesity. *Grn* deficiency blocked elevation of IL-6, an inflammatory cytokine, induced by HFD in blood and adipose tissues. Insulin resistance induced by chronic administration of PGRN was suppressed by neutralizing IL-6 in vivo. Thus, PGRN is a key adipokine that mediates HFD-induced insulin resistance and obesity through production of IL-6 in adipose tissue, and may be a promising therapeutic target for obesity.

INTRODUCTION

Insulin resistance is a characteristic feature of obesity and type 2 diabetes. Adipose tissue is now recognized as not only an energy-storage tissue but also an endocrine tissue that secretes a variety of bioactive substances (adipokines) including adiponectin, resistin, tumor necrosis factor (TNF)-α, interleukin-6 (IL-6), and monocyte chemoattractant protein (MCP)-1 (Shoelson et al., 2007; Waki and Tontonoz, 2007). Defects in adipokine secretion accompanying adipose tissue dysfunction contribute to the pathophysiology of insulin resistance and obesity (Kahn and Flier, 2000). Reduced expression and secretion of adiponectin in obesity promotes the development of systemic insulin resistance by enhancing hepatic gluconeogenesis and suppressing glucose uptake in skeletal muscle (Guilherme et al., 2008; Berg et al., 2001). In contrast, resistin, TNF-α, IL-6 and MCP-1, the levels of which in adipose tissues and blood are elevated in obesity, have been shown to be mediators in progression of insulin resistance (Waki and Tontonoz, 2007).

The relationship between inflammatory process and insulin resistance has recently drawn considerable attention. For example, TNF-α, a proinflammatory cytokine, has been shown to contribute to the development of insulin resistance by altering insulin signaling mediated by activation of the IKK-NFkB and JNK-AP1 signaling pathways (Hotamisligil et al., 1994, 1995; Uysal et al., 1997). On the other hand, glucocorticoids, which are known to have an anti-inflammatory action, also induce insulin resistance in human and animals (Caro and Amatruda, 1982). Dexamethasone, a glucocorticoid, has been reported to impair insulin signaling and insulin-stimulated glucose uptake in adipose tissue, liver, and skeletal muscle (Qi and Rodrigues, 2007). Since TNF-α and dexamethasone both induce insulin resistance despite their opposite inflammatory properties (Hotamisligil et al., 1994; Hotamisligil, 2006; Wellen and Hotamisligil, 2005; Qi and Rodrigues, 2007; van Putten et al., 1985; Turnbow et al., 1994; Sakoda et al., 2000), we reasoned that there might be a common mediator responsible for the cellular basis of insulin resistance induced by TNF-α and dexamethasone. In the present study, we searched for a novel adipokine(s) that

play a key role in developing insulin resistance using 3T3-L1 adipocytes treated with TNF-α or dexamethasone. For this purpose, we utilized a method of differential proteome analysis based on stable isotope labeling of proteins with chemical reagent 2-nitrobenzenesulfenyl chloride (NBSCl) incorporating six ^{13}C ($^{13}C_6$) or six ^{12}C ($^{13}C_0$) in the tryptophan residues (Kuyama et al., 2003; Matsuo et al., 2009). The NBS method has an advantage in reducing the complexity of the analysis because the method targets only peptides that contain tryptophan, which is the least abundant amino acid but is widespread in proteins (Matsuo et al., 2009), and has been used successfully for differential expression analysis in clinical samples (Watanabe et al., 2008; Okamura et al., 2008).

We applied differential proteome analysis using the NBS-based method to search for novel adipokines and identified progranulin (PGRN) as a candidate. PGRN, also known as proepithelin, granulin/epithelin precursor (GEP) or PC cell-derived growth factor (PCDGF), was originally discovered as an acrosomal glycoprotein, named acrogranin, which is synthesized during guinea pig spermatogenesis (Anakwe and Gerton, 1990). PGRN is a 68-88 kDa secreted protein having seven and one-half granulin (GRN) motifs connected by short linker domains (He and Bateman, 2003). It is expressed widely in tissues, especially at high levels in spleen and placenta (Bateman and Bennett, 1998). PGRN has been shown to be a pluripotent growth factor that mediates cell-cycle progression, tumorigenesis, and wound healing (He and Bateman, 2003). PGRN is also implicated in various disease states in humans, including cancers of the breast and ovaries (He and Bateman, 2003), neurodegenerative diseases such as frontotemporal dementia (Cruts and Van Broeckhoven, 2008), and rheumatoid arthritis (Tang et al., 2011).

In the course of this study, it was reported that serum PGRN concentrations in patients with type 2 diabetes are higher than those in normal subjects (Youn et al., 2009). However, the role of PGRN in insulin resistance and obesity remains unknown. In the present study, we found that PGRN is a key adipokine that mediates high fat diet (HFD)-induced insulin resistance, adipocyte hypertrophy, and obesity through production of IL-6 in adipose tissue and that it is a potential target for treating HFD-induced obesity.

RESULTS

Identification of PGRN as an Adipokine Involved in Insulin Resistance In Vitro

To identify proteins associated with insulin resistance in adipocytes in vitro, differential proteome analysis using the NBS method (Matsuo et al., 2009) was performed in 3T3-L1 adipocytes in which insulin resistance was induced by TNF-α or dexamethasone, as outlined in Figure 1A. Expression levels of proteins in these adipocytes were compared with those in untreated adipocytes. The relative ratio of protein expressions was estimated from the intensity of paired peaks with mass difference of 6 Da derived from $^{13}C_0$ and $^{13}C_6$NBS-tagged peptides in mass spectrum (Figure 1B). Since expression levels of glyceraldehydes-3-phosphate dehydrogenase (GAPDH; aa 308-321; *m/z* 1933.1 [$^{13}C_0$], 1939.1 [$^{13}C_6$]) were not changed by these treatments (Figure S1A available online), we used GAPDH as an internal control. We found that 37 and 43 proteins were upregulated by TNF-α treatment and dexamethasone treatment, respectively, among which 21 proteins are common in the two treatments (Figure S1D). We also found that 11 and 7 proteins were downregulated by TNF-α treatment and dexamethasone treatment, respectively, among which 2 proteins are common in these treatments (Figure S1D). Identification of haptoglobin, serum amyloid A-3 (SAA3) protein precursor, and nicotinamide phosphoribosyltransferase, all of which are known as adipokines to be upregulated by such treatment (Shoelson et al., 2007; Lago et al., 2007; do Nascimento et al., 2004; Chiellini et al., 2002), confirmed the validity of the method (Table S1). After excluding known adipokines among the 23 proteins identified, we confirmed the results of differential proteome analysis on 8 proteins by immunoblot analysis using antibodies currently available. We finally selected progranulin (PGRN) because it is the only protein with both secretory and proinflammatory properties.

PGRN, detected as an NBS-modified peptide pair (*m/z* 1634.70 [$^{13}C_0$], 1640.70 [$^{13}C_6$]), was upregulated in both TNF-α-treated (1.66-fold versus control) and dexamethasone-treated (3.01-fold versus control) adipocytes (Figures 1B and S1C). Using tandem mass spectrometry (MS/MS) (Perkins et al., 1999), the heavier peptide peak (*m/z* 1640.70 [$^{13}C_6$]) was found to match the amino acid sequence (N-LNTGAWGCCPFAK-C) of trypsinized peptide derived from PGRN with a $^{13}C_6$NBS modification of the tryptophan residue (MASCOT score 49, expected *P*-value 0.0018) (Figure S1B). Using immunoblot analysis, we confirmed that PGRN detected as an 80 kDa protein was significantly increased under both conditions (Figure S1E).

Induction of PGRN expression by TNF-α or dexamethasone was completely blocked by pioglitazone (Figure 1C), a peroxisome proliferators-activated receptor (PPAR) γ agonist that improves insulin resistance (Olefsky, 2000). In addition, we found that PGRN expression decreased with differentiation of the cells (Figure 1D), as assessed by Pref-1, PPARγ, and FAPB4. These results indicate that PGRN expression is associated strongly with insulin resistance at cell level.

PGRN Has a Causative Role in Insulin Resistance In Vivo

We investigated the role of PGRN in insulin resistance in vivo. Among liver, skeletal muscle, and adipose tissues, which are the major target tissues of insulin, PGRN was expressed at high levels in epididymal fat, at moderate levels in mesenteric fat, and at low levels in liver in wild-type mice but was not expressed in skeletal muscle (Figure 2A). PGRN levels were significantly increased in adipose tissues and liver by HFD but not in skeletal muscle (Figures 2A, S2A, and S2B). *Grn* (the gene symbol of PGRN) was also expressed in leukocytes, spleen, and lung, which abundantly contain immune cells, but was not increased by HFD in these cells and tissues (Figure 2B). Immunohistochemistry of epididymal fat revealed PGRN to be present in adipose tissue (Figure 2C) but the cellular distribution was not clear. Therefore, we performed immunoblot analysis of adipocytes and stromal vascular fraction (SVF) separated from epididymal fat and found the presence of PGRN in both adipocytes and stroma (Figure 2D). Expression levels of PGRN were significantly increased by HFD in both fractions (Figure 2D).

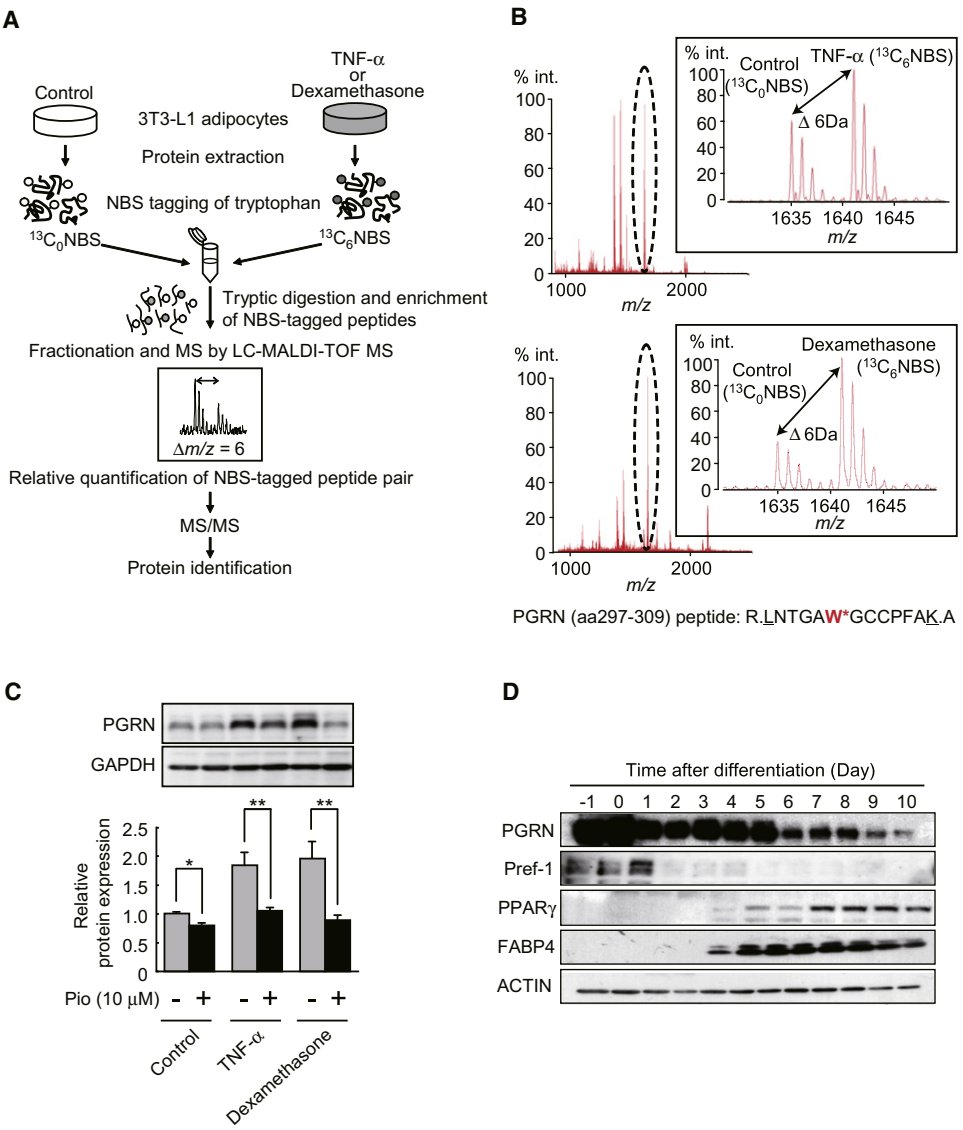

Figure 1. Proteome Analysis of 3T3-L1 Adipocytes Treated with TNF-α or Dexamethasone

(A) Outline of NBS method for differential proteome analysis in 3T3-L1 adipocytes. Proteins from untreated adipocytes were tagged with $^{13}C_0$NBS reagents and those from TNF-α-treated or dexamethasone-treated were tagged with $^{13}C_6$NBS reagents. Relative quantification of the NBS-tagged proteins in the two samples was performed from the MS spectra; proteins were then identified by a database search using queries based on data from the MS/MS spectra.

(B) MS spectrum of NBS proteome analysis. Inset shows $^{13}C_0$NBS- and $^{13}C_6$NBS-tagged peptide (LNTGAWGCCPFAK) from PGRN. The asterisk shown in the peptide sequence indicates the tryptophan residue with a NBS modification.

(C) Effect of pioglitazone (Pio) on PGRN expression in 3T3-L1 adipocytes treated with TNF-α or dexamethasone. Quantitative data are presented as means ± SEM from three independent experiments. *$p < 0.05$; **$p < 0.01$ (Student's unpaired t-test).

(D) Changes in PGRN expression during adipocyte differentiation. The differentiation of 3T3-L1 preadipocytes were initiated by addition of differentiation medium at Day 0. PGRN, Pref-1, PPARγ, FABP4, and ACTIN expressions were determined by immunoblot analysis. Data are representative of three independent experiments.

We then examined *Grn* expression in *ob*/*ob* mice, a well-characterized obese and insulin resistance model (Friedman and Halaas, 1998). *Grn* expression in *ob*/*ob* mice was upregulated in both peritoneal and subcutaneous white adipose tissues (WAT) but not in brown adipose tissue (BAT), as compared with that of *ob*/+ mice (Figure 2E, left). Serum PGRN levels of *ob*/*ob* mice were also higher than those of *ob*/+ mice (Figure 2E, right). Immunohistochemistry of epididymal fat revealed that PGRN was detected predominantly in macrophages (as assessed by Mac-3 costaining) and also was present in the cytoplasm of adipocytes (Figure 2F).

ob/*ob* mice treated with pioglitazone exhibited a significant improvement of glucose tolerance (Figure S2D) and increases in expressions of TZD/PPARγ-dependent genes in adipose tissues (Table S2) but no significant change in body weight (Figure S2C). Under these conditions, *Grn* expressions in both

peritoneal and subcutaneous WAT but not in BAT were decreased significantly (Figure 2G, left). Pioglitazone also normalized serum PGRN levels (Figure 2G, right). These results indicate that PGRN levels in both adipose tissues and blood are associated with insulin resistance and obesity in vivo.

To determine whether PGRN causes insulin resistance in vivo directly, recombinant mouse PGRN (rmPGRN) was administrated intraperitoneally to wild-type (WT) mice under standard diet (SD) condition. We found that serum PGRN levels increased about 2.4-fold within 1 hr after administration and were kept constant for 24 hr onward (Figure S2E); we also found that PGRN levels increased about 2.0–2.5-fold after treatment with rmPGRN for 14 days (Figure S2F). This level of increased serum PGRN is similar to that observed in obese (*ob*/*ob*) mice (Figure 2G, right). Under these conditions, the fasting insulin level in the mice tended to increase (Figure S2I) despite no change in either body weight or blood glucose level (Figures S2G, and S2H). We also found that WT mice treated with rmPGRN for 14 days exhibited insulin resistance, as assessed by insulin tolerance test (ITT) (Figure 2H). Thus, PGRN has a causative role in insulin resistance in vivo. These findings indicate that PGRN is associated with insulin resistance and obesity and that PGRN directly causes insulin resistance in vivo.

Ablation of *Grn* Prevents HFD-Induced Obesity and Insulin Resistance In Vivo

To clarify the physiological and pathophysiological roles of PGRN directly, we utilized *Grn* deficient ($Grn^{-/-}$) mice (Kayasuga et al., 2007). The body weight of $Grn^{-/-}$ mice fed SD was similar to that of WT mice (Figure 3A,top left), whereas the body weight of $Grn^{-/-}$ mice fed HFD was significantly lower than that of WT mice (Figure 3A, top right), despite similar food intake (Figure 3A, bottom). In addition, $Grn^{-/-}$ mice fed HFD exhibited a marked reduction in deposition of peritoneal fat compared to WT mice (Figure 3C, left) as well as in fat mass of both visceral and subcutaneous fat pad (Figure 3B). Immunohistochemistry revealed that the size of adipocytes in epididymal fat pads of $Grn^{-/-}$ mice was significantly smaller than that of WT mice (Figures 3C, middle, and 3D) and that infiltration of mac-3 positive inflammatory cells was significantly less in $Grn^{-/-}$ mice than that in WT mice under HFD condition (Figures 3C,right, and 3E). In addition, glucose intolerance induced by HFD was improved in $Grn^{-/-}$ mice with a decrease in serum insulin levels (Figures 3F and S3A), suggesting enhanced insulin sensitivity in $Grn^{-/-}$ mice. Indeed, insulin tolerance test confirmed that insulin resistance induced by HFD, which was seen in WT mice, was prevented in $Grn^{-/-}$ mice (Figure 3G). These results indicate that ablation of *Grn* prevents HFD-induced obesity and insulin resistance in vivo.

PGRN Impairs Insulin Signaling in Adipocytes

Since PGRN has been shown to be involved in the PI3K/Akt signaling pathway (He and Bateman, 2003; Youn et al., 2009; Zanocco-Marani et al., 1999; Lu and Serrero, 2001), we reasoned that PGRN might directly affect insulin signaling in 3T3-L1 adipocytes. Although PGRN treatment did not affect phosphorylation of insulin receptor (IR) (Figure 4A), it decreased insulin-stimulated phosphorylation of both insulin receptor substrate (IRS)-1 (Figure 4A) and Akt in a dose-dependent manner (Figure 4B). PGRN treatment also suppressed insulin-stimulated glucose uptake (Figure 4C). To further confirm the involvement of PGRN in insulin signaling, we utilized shRNA against *Grn*. The phosphorylations of both IRS-1 and Akt were increased at basal state and were further increased by insulin treatment in *Grn* knockdown (KD) adipocytes compared to those of respective controls, but the phosphorylation of IR was not changed (Figures 4D and 4E). In addition, *Grn* KD also enhanced insulin-stimulated glucose uptake (Figure 4F). Furthermore, the TNF-α-induced decrement of insulin-stimulated Akt phosphorylation was reduced by *Grn* KD (52% in control versus 24% in KD) (Figure 4G). These results indicate that PGRN in adipocytes impairs insulin signaling downstream of IR and suppresses insulin-stimulated glucose uptake and that PGRN mediates TNF-α-induced insulin resistance at cell level.

PGRN Mediates TNF-α-Induced Insulin Resistance through IL-6 Expression in 3T3-L1 Adipocytes

To clarify the mechanism by which PGRN mediates insulin resistance at cell level, we first examined the expressions of adipogenic genes (*Pparg* and *Cebpa*), adipose-specific genes (*Fabp4* and *Glut4*), and inflammatory adipokines (*Lep*, *Il6*, *Tnf*, and *Ccl2*) that are involved in the development of insulin resistance. Expressions of *Pparg* and *Cebpa* in *Grn* KD adipocytes were decreased significantly compared to control (Figure 5A). Among *Lep*, *Il6*, *Tnf*, and *Ccl2*, which are known to be induced by TNF-α, induction of *Il6* was blocked completely in *Grn* KD 3T3-L1 adipocytes (Figure 5A). IL-6 has been reported to induce insulin resistance through JAK/STAT signaling and suppression of cytokine signaling-3 (SOCS3) in both adipocytes and hepatocytes (He et al., 2002; Rotter et al., 2003; Fasshauer et al., 2004; Ueki et al., 2004; Emanuelli et al., 2001; Howard and Flier, 2006). We found that PGRN induced both *Il6* and *Socs3* expression in a dose-dependent manner (Figures 5B and 5C). In addition, induction of STAT3 phosphorylation and *Socs3* expression by TNF-α were also abolished in *Grn* KD adipocytes (Figures 5D and 5E). These results indicate that PGRN promotes IL-6 expression in adipocytes and suggest that the resultant increase in IL-6 enhances SOCS3 expression through activating JAK-STAT signaling, leading to insulin resistance in adipocytes.

PGRN Mediates HFD-Induced Insulin Resistance through IL-6 Expression in Adipose Tissue In Vivo

We then examined expressions of the genes involved in adipocyte hypertrophy and inflammation in adipose tissue. In epididymal fat of $Grn^{-/-}$ mice, expressions of *Pparg* and *Cebpa*, *Fabp4*, *Glut4*, and *Adipoq* decreased significantly compared to those in WT mice (Figure 6A). HFD-induced elevations of inflammatory markers *Il6*, *Tnf*, and *Emr1* were found in WT mice but not in $Grn^{-/-}$ mice (Figure 6A).

Among *Il6*, *Tnf*, and *Ccl2* induced by HFD, induction of *Il6* was blocked almost completely in adipose tissue of $Grn^{-/-}$ mice (Figure 6A), as was found in *Grn* KD adipocytes (Figure 5A). In addition, HFD-induced elevation of serum IL-6 concentration was also blocked markedly in $Grn^{-/-}$ mice (Figure 6B). Moreover, HFD-induced *Socs3* expressions were completely diminished in both epididymal fat and liver in $Grn^{-/-}$ mice (Figures 6C and 6D). Because expression of *Il6* in liver was not changed by HFD (Figure 6E), HFD-induced SOCS3 expression is likely to be mediated by IL-6 derived from adipose tissue.

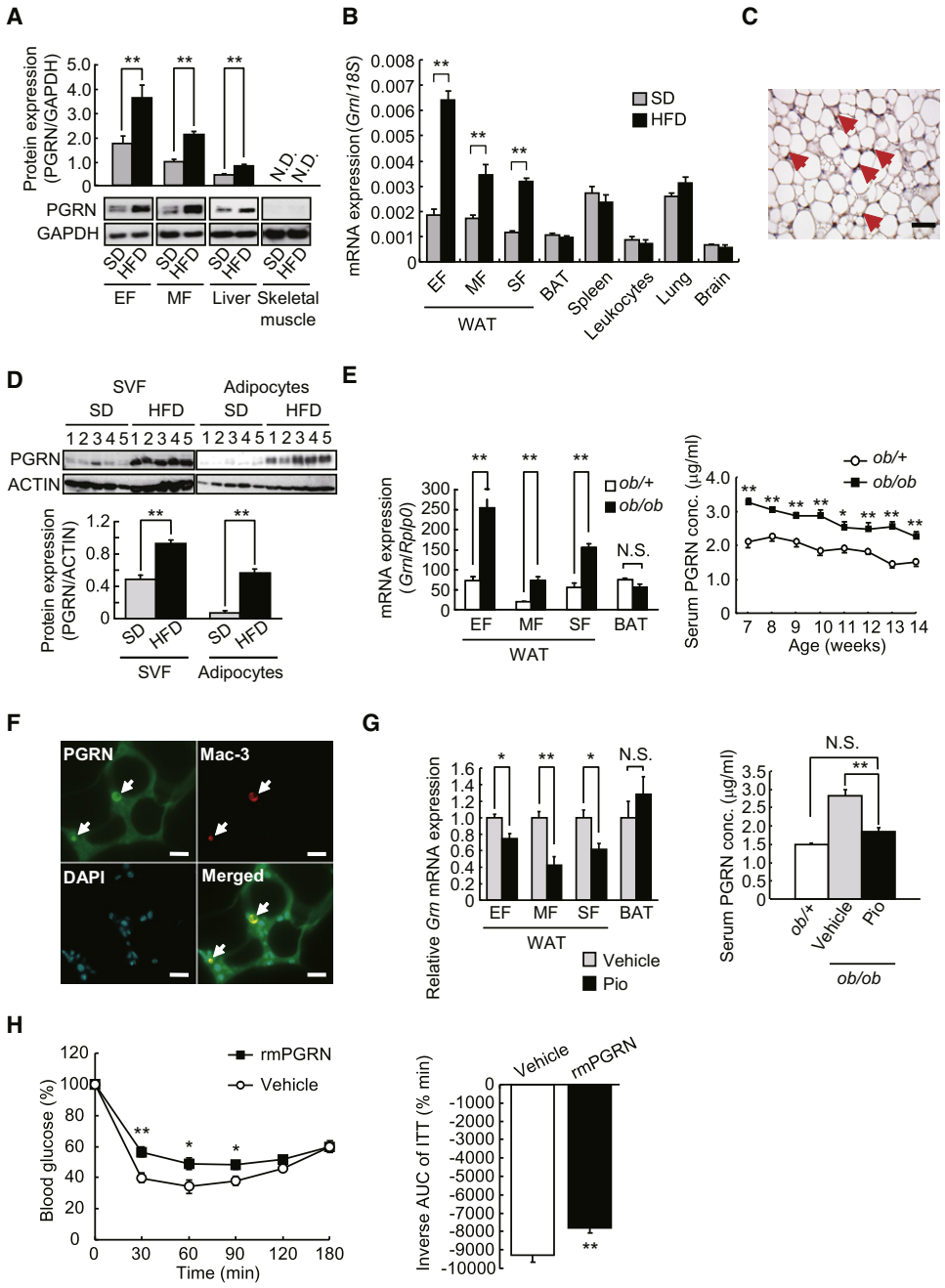

Figure 2. Relationship between PGRN and Insulin Resistance In Vivo

(A) Immunoblot analysis of PGRN in epididymal fat (EF; 6 μg/lane, n = 5), mesenteric fat (MF; 6 μg/lane, n = 5), liver (12 μg/lane, n = 5), and skeletal muscle (12 μg/lane, n = 5) in 26-week-old C57BL/6J mice fed standard diet (SD) or high fat diet (HFD).

(B) mRNA expression of *Grn* in EF, MF, subcutaneous fat (SF), brown adipose tissue (BAT), spleen, leukocytes, lung, and brain in 23-week-old C57BL/6J mice (n = 5) fed SD or HFD.

(C) Immunohistochemistry of PGRN in EF of 11-week-old C57BL/6J mice on SD. Immunoreactivities of PGRN (red arrow) are shown. Scale bar, 50 μm.

(D) Immunoblot analysis of PGRN in stromal vascular fraction (SVF) and adipocytes from EF of 33-week-old C57BL/6J mice (SD, n = 5; HFD, n = 5).

(E) PGRN levels in adipose tissues (left) and serum (right) of *ob*/+ (n = 5) and *ob*/*ob* (n = 5) mice. *Grn* expression in EF, MF, SF, and BAT at 10-week-old were quantified by quantitative real-time RT-PCR analysis, and serum concentrations of PGRN were measured by ELISA assay.

(F) Immunofluorescent staining of PGRN and mac-3, and nuclear counterstaining with DAPI in EF of 14-week-old *ob*/*ob* mice. Arrows indicate mac-3 positive cells. Scale bars, 25 μm.

(G) Effect of pioglitazone (Pio) on PGRN levels in adipose tissues (left) and serum (right) of *ob*/*ob* mice. Pio (n = 5) or vehicle (n = 4) was administered to *ob*/*ob* mice for 7 days. *Grn* expressions in adipose tissues and serum concentrations of PGRN were quantified by quantitative real-time RT-PCR analysis and ELISA assay, respectively.

Neutralizing IL-6 Improves PGRN-Induced Insulin Resistance In Vivo

To ascertain that IL-6 mediates PGRN-induced insulin resistance in vivo, we utilized neutralizing antibody against IL-6. We found that PGRN level was increased about 2.1-fold after chronic treatment of WT mice fed SD with rmPGRN (20 μg/day) once daily for 3 weeks (Figure S4A). Under this condition, the increased fasting serum insulin level in the mice treated with rmPGRN tended to be decreased by neutralizing antibody against IL-6 despite no change in either body weight or blood glucose level (Figures S4B–S4D). Importantly, ITT reveals that insulin resistance induced by rmPGRN was significantly improved by neutralizing antibody against IL-6 (Figure 7) without change in body weight (Figure S4B), indicating that IL-6 is a mediator of PGRN-induced insulin resistance in vivo.

DISCUSSION

In the present study, we found that PGRN is a key adipokine mediating HFD-induced insulin resistance and obesity through IL-6 in adipose tissues. Despite an extensive search for novel adipokines, PGRN has not been reported as an adipokine to date. The NBS method used here has an advantage in reducing the complexity of analysis by targeting peptides containing tryptophan, which is the least abundant amino acid but is widespread in proteins (Matsuo et al., 2009), and has permitted identification of PGRN as an adipokine.

Proinflammatory adipokines, which are secreted from adipocytes and/or macrophages in adipose tissue, induce a low-grade chronic inflammatory state that plays a critical role in insulin resistance associated with obesity (Hotamisligil, 2006; Wellen and Hotamisligil, 2005; Weisberg et al., 2003; Xu et al., 2003). However, the molecular basis for adipocyte hypertrophy and the inflammation process underlying obesity is not fully understood. PGRN caught our attention because it is a secreted protein associated with proinflammatory properties and, therefore, is a strong candidate for an adipokine involved in insulin resistance. PGRN has been characterized as the precursor of granulins (GRNs), some of which have been shown to modulate inflammation and wound repair (He and Bateman, 2003). The physiological and pathophysiological functions of PGRN are complex: PGRN has both anti-inflammatory and proinflammatory properties (Zhu et al., 2002; Kessenbrock et al., 2008; He and Bateman, 2003). It has been suggested that the full-length form of the protein has trophic and anti-inflammatory activity, whereas proteolytic cleavage generates GRNs that promote inflammatory activity (Eriksen and Mackenzie, 2008). However, we found that PGRN levels were increased in the insulin resistant state both in vivo and in vitro and that PGRN induced the expression of IL-6, a proinflammatory adipokine. Accordingly, PGRN in adipose tissues may well participate in chronic inflammation associated with insulin resistance and obesity. A recent study has shown that PGRN binds to TNF receptor and prevents mice from inflammatory arthritis by blocking interaction with TNF-α (Tang et al., 2011). Thus, it is possible that PGRN has dual roles in inflammation and exerts proinflammatory or anti-inflammatory function in different tissues.

In the present study, we also found that ablation of PGRN protected against HFD-induced obesity and insulin resistance in vivo. Although $Grn^{-/-}$ mice were originally reported to exhibit offensive behavior against intruders, the mice did not show hyperactivity under SD condition (Kayasuga et al., 2007). In addition, neither energy metabolism nor locomotor activity under HFD condition was investigated in their study. To determine whether hyperactive behavior and/or energy expenditure contributed to the development of obesity in $Grn^{-/-}$ mice, we measured locomotor activity and performed respiratory gas analysis before the development of obesity in these mice. $Grn^{-/-}$ mice exhibited neither hyperactivity (Figure S3B) nor increased energy expenditure (Figures S3C–S3I) under SD or HFD condition. It is unlikely, therefore, that the protective phenotype against HFD-induced obesity is due to hyperactivity. Interestingly, the respiratory quotient in $Grn^{-/-}$ mice fed HFD was significantly lower at dark phase, suggesting that ablation of PGRN suppressed HFD-induced obesity by consuming lipids more preferentially than carbohydrate (Figure S3H).

We have also found that PGRN induces insulin resistance through IL-6 both in vivo and in vitro. It has been hypothesized that chronic increase of IL-6 plays a role in causing insulin resistance associated with obesity. IL-6 alters insulin signaling differently in various tissues (Mooney, 2007). The IL-6 / STAT3 pathway is required for the action of insulin signaling in the brain on hepatic gluconeogenesis (Wallenius et al., 2002; Inoue et al., 2006). Therefore, IL-6 has both central and peripheral roles in metabolism and its effects on systemic insulin resistance are complex. However, IL-6 expression in adipose tissue is known to contribute to developing chronic inflammatory states, such as obesity (Senn et al., 2002; Fried et al., 1998; Shoelson et al., 2007). In addition, it has been shown that circulating IL-6 is elevated in obese, diabetic subjects (Pickup et al., 1997; Kern et al., 2001) and that adipose tissue is a major site of IL-6 secretion, accounting for 15%–35% of circulating levels (Fried et al., 1998; Mohamed-Ali et al., 1997). Considered with our finding that adipose tissue is a major source of increased PGRN in the blood of mice fed HFD, PGRN may well induce IL-6 expression in adipose tissues in obesity.

The mechanisms by which IL-6 inhibits insulin signaling have been studied extensively in adipocytes and hepatocytes (Mooney, 2007). IL-6 has been shown to attenuate insulin signaling, which is mediated by increasing SOCS3 expression through activation of JAK-STAT signaling in adipocytes and hepatocytes (Ueki et al., 2004; Shi et al., 2004; Senn et al., 2003; Emanuelli et al., 2001). SOCS3 impairs tyrosine phosphorylation of IRS-1 by direct interaction and promotes proteasomal degradation of IRS-1 (Ueki et al., 2004; Emanuelli et al., 2001).

(H) Induction of insulin resistance by administration of recombinant PGRN in vivo. Recombinant mouse PGRN (rmPGRN, i.p. 20 μg/day) or PBS (vehicle) was administered to C57BL/6J mice once daily for 14 days (n = 7) under SD condition. Insulin sensitivity was assessed by insulin tolerance test (ITT) (left). Blood glucose levels were determined at the indicated times after intraperitoneal injection of insulin (0.5 IU/kg). Inverse area under curve (AUC) of ITT was shown (right). All data are means ± SEM. *$p < 0.05$; **$p < 0.01$ in (A), (B), (D), (E), left of (G), (H) (Student's unpaired t-test) and in right (G) (Dunnet's method); N.S., not significant.

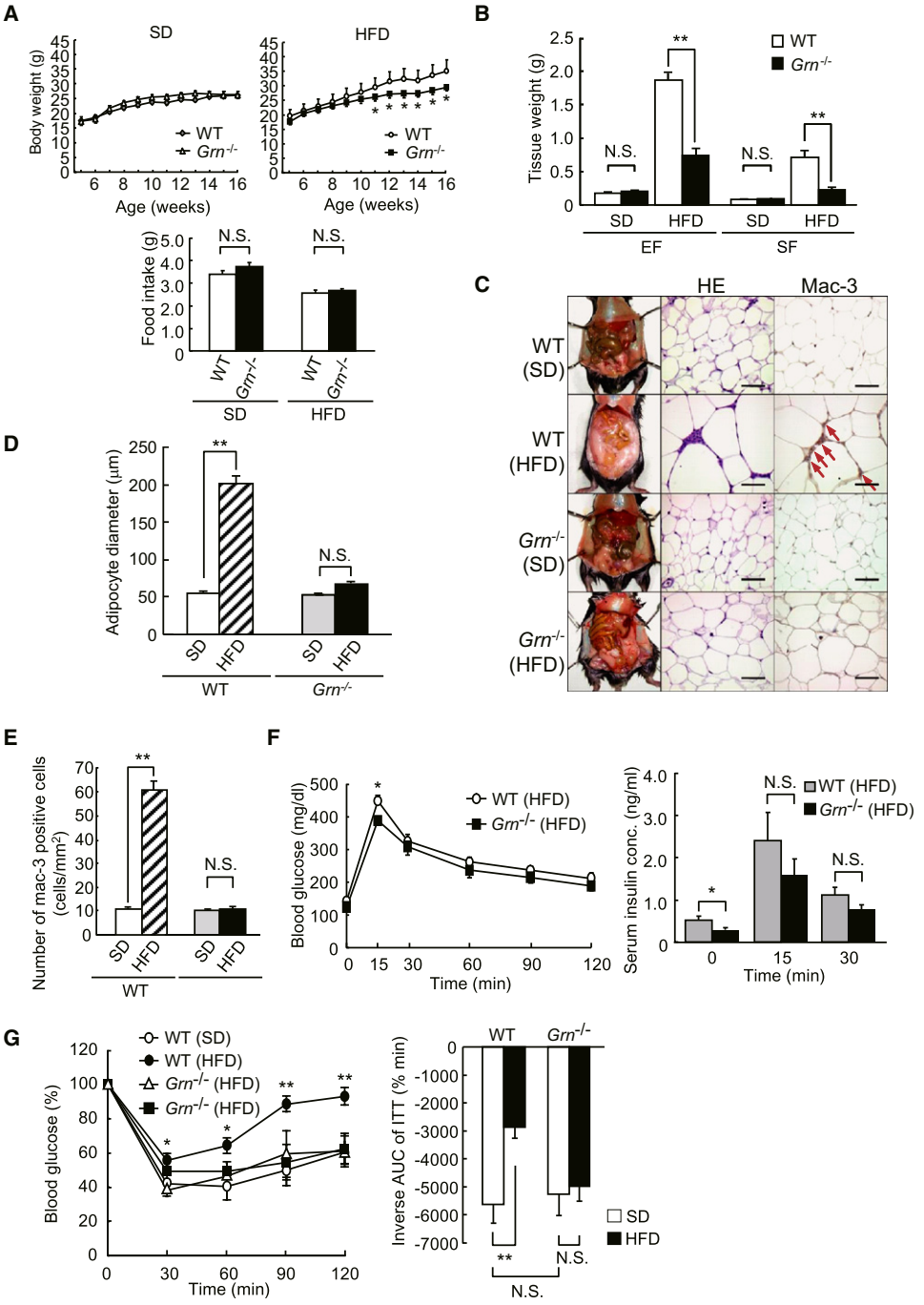

Figure 3. Prevention of High Fat Diet-Induced Insulin Resistance, Adipocyte Hypertrophy, and Obesity by Ablation of *Grn* In Vivo

(A) Changes in body weight and food consumption on SD or HFD. Changes in body weights in WT (SD, n = 8, HFD, n = 8) and $Grn^{-/-}$ (SD, n = 5, HFD, n = 9) mice were measured. Food consumptions in WT (n = 11) and $Grn^{-/-}$ (n = 9) mice fed SD or HFD for 1 week are shown as food intake (g) per day.

(B) Tissue weight of WATs in WT (SD, n = 8; HFD, n = 8) and $Grn^{-/-}$ mice (SD, n = 8; HFD, n = 7).

(C-E) Gross appearance (C left), histology (H&E staining: C middle, mac-3 immunostaining: C right), adipocyte diameter (n = 100) (D), and number of mac-3 positive cells (n = 10) (E) in epididymal fat of WT and $Grn^{-/-}$ mice. Red arrows indicate mac-3 positive cells. Scale bars, 50 μm.

(F) Oral glucose tolerance test. Blood glucose (left) and serum insulin (right) levels in WT mice (SD, n = 8; HFD, n = 10) and $Grn^{-/-}$ mice (SD, n = 5; HFD, n = 9) were determined at the indicated times after oral administration of glucose.

(G) Insulin tolerance test (ITT). Blood glucose levels in WT (SD, n = 8; HFD, n = 9) and $Grn^{-/-}$ (SD, n = 5; HFD, n = 9) mice were determined at the indicated times after intraperitoneal injection of insulin (0.3 IU/kg) (left). Insulin sensitivity was assessed by inverse AUC of ITT (right).

All data are means ± SEM. *p < 0.05; **p < 0.01 in (A), (B), (D), (E), (F) (Student's unpaired t-test), and in (G), compared with WT mice fed SD (Dunnet's method); N.S., not significant.

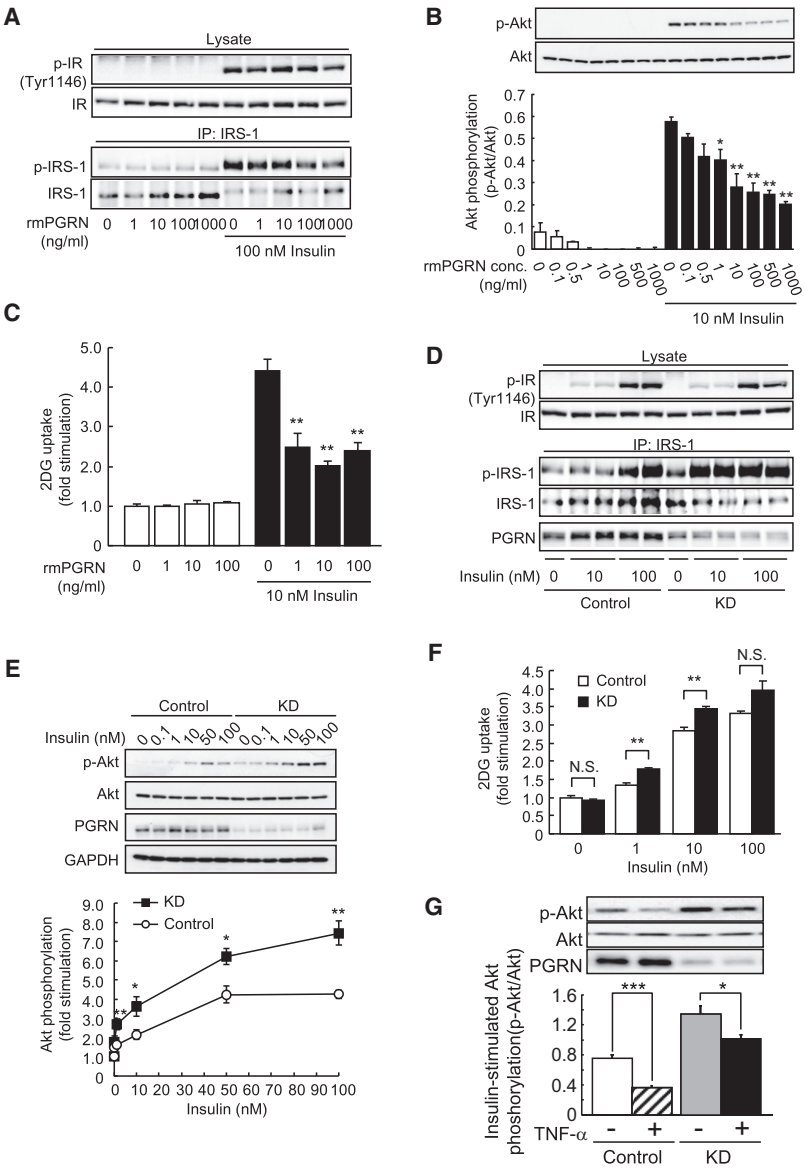

Figure 4. Inhibition of Insulin Signaling by PGRN in 3T3-L1 Adipocytes

(A) Effects of exogenous PGRN on IR and IRS-1 phosphorylation. 3T3-L1 adipocytes were treated with various concentrations of recombinant mouse PGRN protein (rmPGRN) for 20 hr and subsequently stimulated with 100 nM of insulin for 10 min. Activation of insulin signaling was then assessed by phosphorylation of IR (Tyr1146) and tyrosine phosphorylation of immunoprecipitated (IP) IRS-1.

(B) Effect of exogenous PGRN on Akt phosphorylation (n = 4). 3T3-L1 adipocytes were treated with various concentrations of rmPGRN for 4 hr and subsequently stimulated with 10 nM of insulin for 10 min. Activation of insulin signaling was then assessed by phosphorylation of Akt (Ser743).

(C) Effects of exogenous PGRN on glucose uptake. 3T3-L1 adipocytes were treated with various concentrations of rmPGRN for 20 hr and subsequently stimulated with 10 nM of insulin for 10 min (n = 3).

(D) Effects of *Grn* knockdown (KD) on IR and IRS-1 phosphorylation. 3T3-L1 adipocytes were infected with adenovirus carrying shRNA for *Grn* (Grn^{shRNA}) or adenovirus carrying nontarget shRNA (control) at MOI of 100. Activation of insulin signaling was then assessed by phosphorylation of IR (Tyr1146) and tyrosine phosphorylation of immunoprecipitated (IP) IRS-1.

(E) Effect of *Grn* KD on insulin-stimulated Akt phosphorylation. Insulin-stimulated Akt phosphorylation in KD or control cells was analyzed by immunoblot analysis (n = 4).

(F) Effects of *Grn* KD on glucose uptake (n = 3).

(G) Effect of *Grn* KD on the suppression by TNF-α of insulin-stimulated Akt phosphorylation. KD or control cells were treated with 10 ng/ml TNF-α for 16 hr. Insulin-stimulated Akt phosphorylation was then analyzed by immunoblot analysis (n = 4).

All data are means ± SEM. *p < 0.05; **p < 0.01; ***p < 0.0005 in (B), (C) (Dunnet's method) and in (E), (F), (G) (Student's unpaired t-test); N.S., not significant.

Thus, the finding that PGRN in vitro impairs insulin signaling downstream of IR and meditates TNF-α-induced IL-6 expression implicates IL-6 as a mediator of PGRN-induced insulin resistance in adipocytes.

In the present study, we also found that neutralizing antibody against IL-6 improved PGRN-induced insulin resistance in vivo. Treatment with IL-6 enhances hepatic insulin resistance (Klover et al., 2003; Lagathu et al., 2003), while neutralization of IL-6 by administration of antibody specific for IL-6 reduces HFD-induced insulin resistance (Klover et al., 2005). It has been reported also that reduced expression of IL-6 in adipose tissues by adipocyte-specific deficiency of JNK potentiates hepatic insulin sensitivity and prevents mice from the development of insulin resistance by HFD (Sabio et al., 2008). Taken together, these findings suggest that PGRN in adipose tissues triggers systemic insulin resistance by elevating levels of IL-6 in adipose tissues and blood.

SOCS3 has been shown to be a physiological regulator of insulin signaling in both hepatocytes and adipocytes (Rønn et al., 2007). SOCS3 expression was found to be elevated in adipose tissue of obese mice (Emanuelli et al., 2001). In addition, ablation of *Socs3* in liver improved hepatic insulin sensitivity (Torisu et al., 2007; Sachithanandan et al., 2010). Considered together with our present findings, SOCS3 might, therefore, contribute to the development of systemic insulin resistance by PGRN through elevated levels of IL-6.

In conclusion, PGRN is a key adipokine that mediates HFD-induced insulin resistance and obesity through IL-6 and may be a promising therapeutic target for preventing obesity.

EXPERIMENTAL PROCEDURES

Mice

We obtained male C57BL/6J from CLEA Japan (Tokyo, Japan), and *ob/ob* and *ob/+* mice from Charles River Japan (Yokohama, Japan). $Grn^{+/-}$ mice were purchased from RIKEN BioResource Center (BRC) (Tsukuba, Japan). Genotyping of $Grn^{-/-}$ mice was performed as described previously (Kayasuga et al., 2007). C57BL/6J mice were fed HFD from 7 through 33 weeks of age.

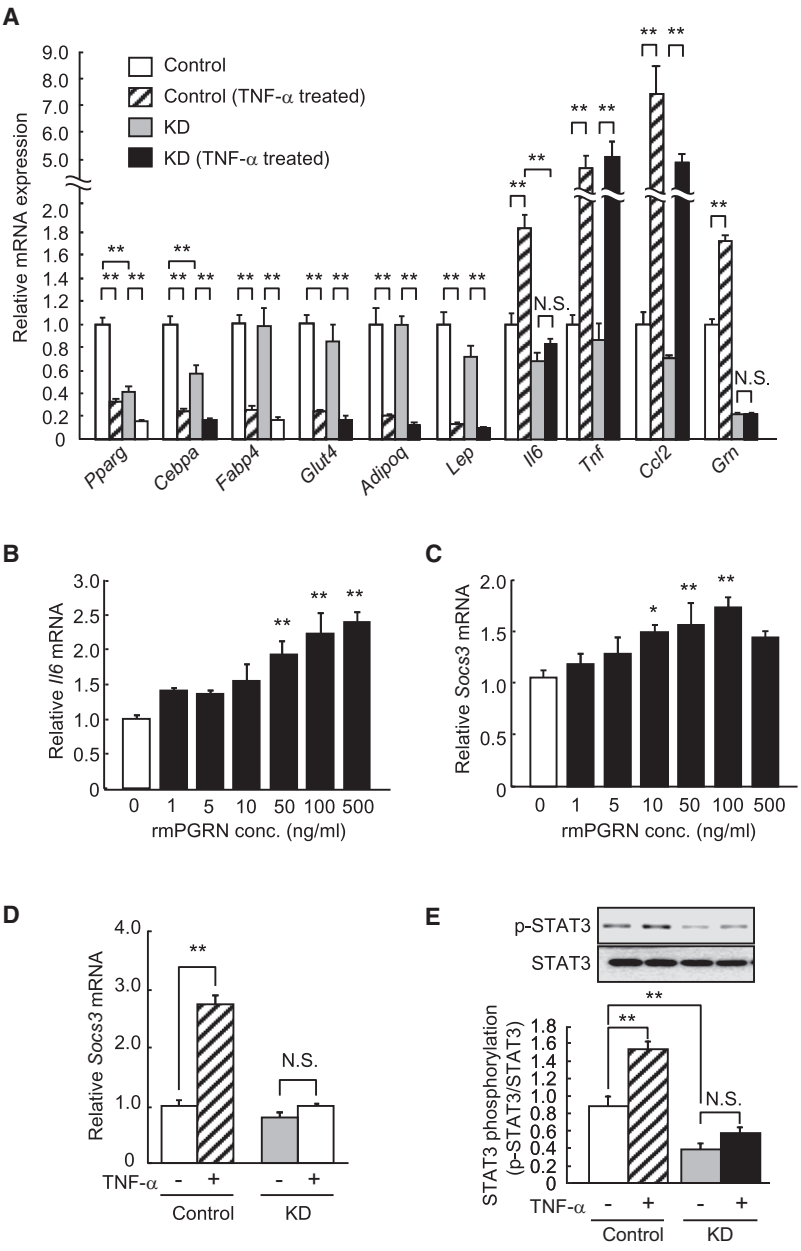

Figure 5. Effects of *Grn* Knockdown or PGRN Treatment on *Il6* and *Socs3* Expressions in 3T3-L1 Adipocytes

(A) Quantitative real-time RT-PCR analysis of various genes in *Grn* KD adipocytes (n = 6). 3T3-L1 adipocytes infected with adenovirus carrying Grn^{shRNA} or adenovirus carrying nontarget shRNA (control) at MOI of 100 were treated with or without 10 ng/ml TNF-α for 16 hr.

(B) Effect of exogenous PGRN on *Il6* mRNA expression. *Il6* expression in 3T3-L1 adipocytes treated with indicated concentrations of recombinant PGRN protein for 16 hr were examined by quantitative real-time RT-PCR analysis (n = 6).

(C) Effect of exogenous PGRN on *Socs3* mRNA expression (n = 6). *Socs3* expression in 3T3-L1 adipocytes treated with indicated concentrations of recombinant PGRN protein for 16 hr were examined by quantitative real-time RT-PCR analysis.

(D) Quantitative real-time RT-PCR analysis of *Socs3* in *Grn* KD adipocytes (n = 6). *Grn* KD and control 3T3-L1 adipocytes were treated as in (A).

(E) Effect of *Grn* KD on TNF-α stimulated STAT3 phosphorylation (n = 6). STAT3 phosphorylation in KD and control 3T3-L1 adipocytes treated as in (A) was analyzed by immunoblot analysis.

All data are means ± SEM. *p < 0.05; **p < 0.01 in (A), (D), and (E) (Tukey-Kramer's method) and in (B) and (C) (Dunnet's method); N.S., not significant.

$Grn^{-/-}$ mice were fed HFD from 5 through 17 weeks of age. The SD (CE-2, CLEA Japan) supplied 4.8% of calories as fat with an energy density of 3.43 kcal/g. The HFD (D12492, Research Diet Inc., NJ) supplied 60% of calories as fat with an energy density of 5.24 kcal/g. Animal care and experimental procedures were approved by the Institutional Animal Care and Use Committee and carried out according to the Kobe University Experimentation Regulations.

Cell Culture

3T3-L1 cells were purchased from the American Tissue Culture Collection (Manassas, VA) and maintained at 37°C in a humidified atmosphere of 5% CO_2–95% air in Dulbecco's modified Eagle's medium (DMEM) containing 5.6 mM glucose (Wako) supplemented with 10% (vol/vol) heat-inactivated newborn calf serum (Invitrogen, Carlsbad, CA). Differentiation medium, which consists of DMEM containing 25 mM glucose supplemented with 10% fetal bovine serum (FBS) (Hyclone, Logan, UT), 0.5 mM isobutylmethylxanthine (IBMX), 5 μg/ml insulin, and 1 μM dexamethasone was added to preadipocytes 2 days after reaching confluence (day 0). On day 3, the medium was replaced with DMEM containing 25 mM glucose, 10% FBS and 5 μg/ml insulin. From day 5 onward, cells were maintained in DMEM containing 25 mM glucose and 10% FBS, with a media change every other day until experimental treatments were initiated. Dexamethasone (20 nM) or TNF-α (4 ng/ml) was added to mature adipocytes at any time from day 8 to day 14 of differentiation. Media containing TNF-α was changed daily for a total incubation period of 4 days. Media containing dexamethasone was changed every other day for a total of 8 days. Cells were then collected by scraping and were lysed in buffer containing 6 M guanidine-HCl, 50 mM Tris-HCl (pH 8.0), 2 mM EDTA, 1 mM phenylmethylsulfonyl fluoride (PMSF), 10 μg/ml leupeptin, and 10 μg/ml aprotinin) for NBS reagent labeling, or in TNE buffer [1% (w/w) Nonidet-P40, 150 mM NaCl, 20 mM Tris-HCl (pH 7.4), 2 mM EDTA, 10 μg/ml leupeptin, 10 μg/ml aprotinin, 5 mM mercaptoethanol, 1 mM PMSF, 1 mM Na_3VO_4, 10 μM Na_2MoO_4, 50 mM NaF] for immunoblot analysis.

NBS Tagging, Peptide Fractionation, and Mass Spectrometry

NBS tagging was performed according to the manufacturer's protocol (^{13}CNBS stable isotope labeling kit-N; Shimadzu Biotech, Kyoto, Japan). Briefly, each cell lysate (each containing 200 μg of protein) was labeled with isotopically $^{13}C_0$NBS or $^{13}C_6$NBS reagent. NBS-tagged proteins were then mixed, reduced, alkylated, and digested by trypsin. NBS-tagged peptides were enriched and separated by reversed-phase liquid choromatography (LC-10ADvp μHPLC System; Shimadzu, Kyoto, Japan) as described previously (Matsuo et al., 2009). Eluates were automatically deposited onto MALDI target plates by the LC spotting system (AccuSpot; Shimadzu). These spotted samples were automatically analyzed by MALDI-TOF MS (AXIMA-CFR Plus or AXIMA-TOF^2; Shimadzu/Kratos, Manchester, UK).

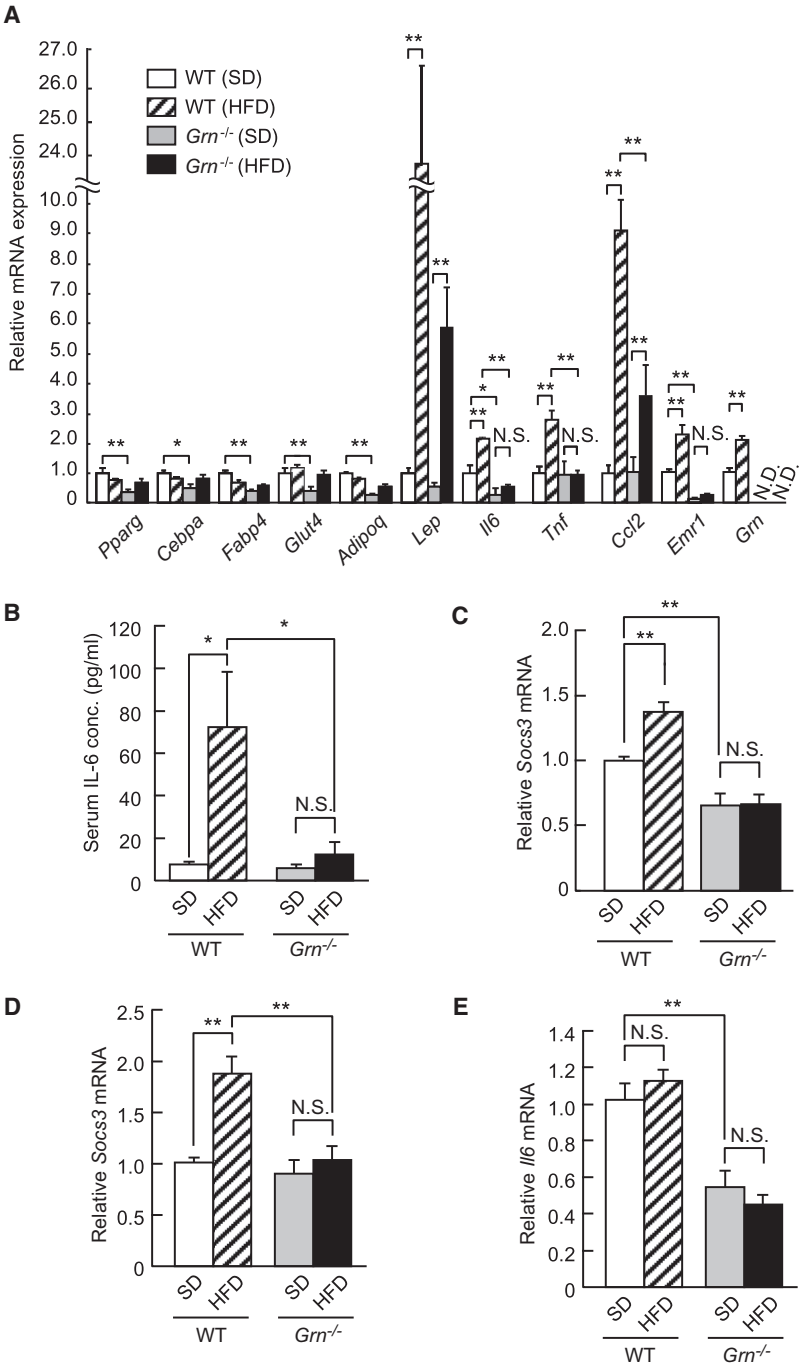

Figure 6. Effects of *Grn* Deficiency on HFD-Induced Elevation of IL-6 and SOCS3 In Vivo

(A) Quantitative real-time RT-PCR analysis of EF of WT (SD, n = 8; HFD, n = 8) and $Grn^{-/-}$ mice (SD, n = 7; HFD, n = 5).

(B) Serum concentrations of IL-6 in WT (SD, n = 19; HFD, n = 27) and $Grn^{-/-}$ mice (SD, n = 15; HFD, n = 22).

(C) Quantitative real-time RT-PCR analysis of *Socs3* in EF of WT (SD, n = 8; HFD, n = 8) and $Grn^{-/-}$ mice (SD, n = 7; HFD, n = 5).

(D) Quantitative real-time RT-PCR analysis of *Socs3* in liver of WT (SD, n = 6; HFD, n = 8) and $Grn^{-/-}$ mice (SD, n = 7; HFD, n = 7).

(E) Quantitative real-time RT-PCR analysis of *Il6* in liver of WT mice (SD, n = 6; HFD, n = 8) and $Grn^{-/-}$ mice (SD, n = 7; HFD, n = 7).

All data are means ± SEM. *p < 0.05; **p < 0.01 (Tukey-Kramer's method); N.S., not significant.

MASCOT Distiller. The Mascot search parameters were as follows: trypsin digestion allowing up to 2 missed cleavages, fixed modifications of $^{13}C_0$NBS (or $^{13}C_6$NBS) (W) and carbamidomethyl (C), variable modifications of oxidation (M), peptide tolerance of 0.3 Da, and MS/MS tolerance of 0.5 Da. Search results with p values less than 0.05 were judged as positive identifications.

Fractionation of Epididymal White Adipose Tissue

Epididymal white adipose tissues (WAT) dissected from mice were minced and digested with 2 mg/ml collagenase P (Roche, Mannheim, Germany) in DMEM containing 1% BSA and antibiotics for 45 min at 37°C. The digested tissues were passed through a nylon mesh filter (pore size, 150 μm) to remove undigested material, and the filtrates were centrifuged for 5 min at 250 x g. Floating cells and the pellet was recovered as the mature adipocyte fraction and the SVF, respectively, and washed twice with phosphate buffered-saline (pH 7.4).

Treatment of *ob/ob* Mice with Pioglitazone

Pioglitazone (30 mg/kg) or vehicle (0.25% carboxymethyl cellulose) was administered orally to 13-week-old *ob/ob* mice once daily for 7 consecutive days.

Preparation of Recombinant PGRN

Mouse PGRN (mPGRN) cDNA clone, MGC Image clone, was purchased from Invitrogen. pCAGIPuro-FLAG-mPGRN was constructed by subcloning the insert encoding the mPGRN without signal peptide (amino acid 18 to 589), into pCAGIPuro-FLAG (Satoh-Horikawa et al., 2000). To prepare CHO-K1 cells stably expressing the FLAG-tagged mPGRN, CHO-K1 cells were transfected with pCAGIPuro-FLAG-mPGRN construct by electroporation. Stably expressed cells were maintained in CD OptiCHO medium (Invitrogen) supplemented with 10 μg/ml puromycin (SIGMA), 4 mM GlutaMAX (Invitrogen) 1 × HT supplement (Invitrogen), and 10 μg/ml insulin (SIGMA). Culture supernatants were collected and subjected to anti-FLAG M1 agarose affinity gel (SIGMA) column. The column was washed with 50 mM Tris-HCl (pH7.5), 150 mM NaCl and 1 mM $CaCl_2$, and then eluted with 50 mM Tris-HCl (pH7.5), 150 mM NaCl, and 2 mM EDTA. The eluted proteins were dialyzed against PBS.

Relative Quantification and Identification of Differentially Expressed Proteins

Relative quantification between $^{13}C_0$NBS- and $^{13}C_6$NBS-tagged peptides was performed using the proteome analysis assistant software for relative quantification, TWIP Version 1.0 (DYNACOM, Chiba, Japan), referring to a monoisotopic mass list from MASCOT Distiller Ver. 1.1.2 (Matrix Science, London, UK) as described previously (Matsuo et al., 2009). Threshold values of $^{13}C_6/^{13}C_0$ ratios in NBS-tagged peptide pairs were set to either larger than 1.25 or less than 0.8. Candidate peptides having significant difference in peptide pair ratios were selected and further subjected to MS/MS analysis (AXIMA-QIT-TOF MS; Shimadzu / Kratos). Proteins were identified by MASCOT MS/MS Ion Search algorithm (Version 2.0; Matrix Science) using mass lists generated by

Statistical Analysis

The data are expressed as means ± SEM. Comparisons were made using Student's t-test, Dunnet's method or Tukey-Kramer's method as indicated in the legends. A *P* value of < 0.05 was considered statistically significant.

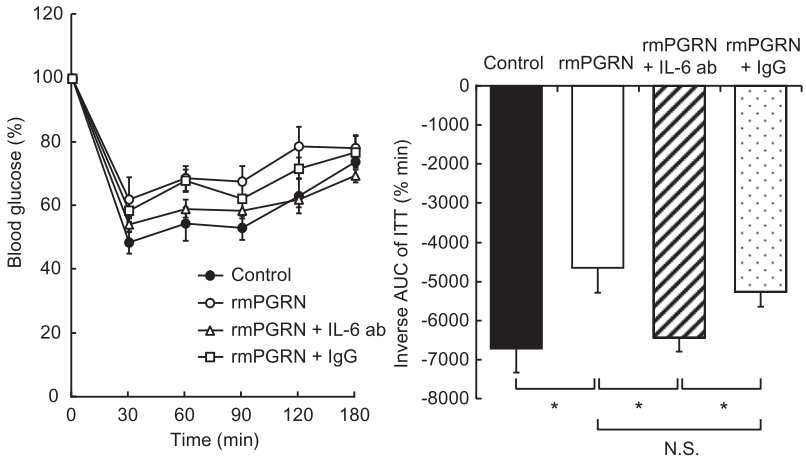

Figure 7. Effects of Neutralizing Antibody against IL-6 on Insulin Resistance Induced by PGRN In Vivo

Recombinant mouse PGRN (rmPGRN, i.p. 20 μg/day) or PBS (control) was administered to C57BL/6J mice once daily for 21 days (n = 7). Neutralizing antibody against IL-6 (n = 7) or IgG (n = 6) was administered to the mice 72 hr before ITT. Insulin sensitivity was assessed by inverse AUC (right) of ITT (left) (insulin injection: 0.3 IU/kg).

All data are means ± SEM. *p < 0.05 (Tukey-Kramer's method); N.S., not significant.

SUPPLEMENTAL INFORMATION

Supplemental Information includes Supplemental Experimental Procedures, four figures, and two tables and appears with this article online at doi:10.1016/j.cmet.2011.12.002.

ACKNOWLEDGMENTS

We thank for G.K. Honkawa for assistance with the manuscript. This study was supported by a CREST grant from the Japan Science and Technology Agency and Grant-in-Aid for Scientific Research and by grants for the Kobe Translational Research Cluster, the Knowledge Cluster Initiative, and the Global Centers of Excellence Program "Global Center of Excellence for Education and Research on Signal Transduction Medicine in the Coming Generation" from the Ministry of Education, Culture, Sport, Science and Technology, Japan.

Received: November 4, 2010
Revised: September 23, 2011
Accepted: December 2, 2011
Published: January 3, 2012

REFERENCES

Anakwe, O.O., and Gerton, G.L. (1990). Acrosome biogenesis begins during meiosis: evidence from the synthesis and distribution of an acrosomal glycoprotein, acrogranin, during guinea pig spermatogenesis. Biol. Reprod. *42*, 317–328.

Bateman, A., and Bennett, H.P.J. (1998). Granulins: the structure and function of an emerging family of growth factors. J. Endocrinol. *158*, 145–151.

Berg, A.H., Combs, T.P., Du, X., Brownlee, M., and Scherer, P.E. (2001). The adipocyte-secreted protein Acrp30 enhances hepatic insulin action. Nat. Med. *7*, 947–953.

Caro, J.F., and Amatruda, J.M. (1982). Glucocorticoid-induced insulin resistance: the importance of postbinding events in the regulation of insulin binding, action, and degradation in freshly isolated and primary cultures of rat hepatocytes. J. Clin. Invest. *69*, 866–875.

Chiellini, C.A., Bertacca, A., Novelli, S.E., Görgün, C.Z., Ciccarone, A., Giordano, A., Xu, H., Soukas, A., Costa, M., Gandini, D., et al. (2002). Obesity modulates the expression of haptoglobin in the white adipose tissue via TNFalpha. J. Cell. Physiol. *190*, 251–258.

Cruts, M., and Van Broeckhoven, C. (2008). Loss of progranulin function in frontotemporal lobar degeneration. Trends Genet. *24*, 186–194.

do Nascimento, C.O., Hunter, L., and Trayhurn, P. (2004). Regulation of haptoglobin gene expression in 3T3-L1 adipocytes by cytokines, catecholamines, and PPARgamma. Biochem. Biophys. Res. Commun. *313*, 702–708.

Emanuelli, B., Peraldi, P., Filloux, C., Chavey, C., Freidinger, K., Hilton, D.J., Hotamisligil, G.S., and Van Obberghen, E. (2001). SOCS-3 inhibits insulin signaling and is up-regulated in response to tumor necrosis factor-α in the adipose tissue of obese mice. J. Biol. Chem. *276*, 47944–47949.

Eriksen, J.L., and Mackenzie, I.R. (2008). Progranulin: normal function and role in neurodegeneration. J. Neurochem. *104*, 287–297.

Fasshauer, M., Kralisch, S., Klier, M., Lossner, U., Bluher, M., Klein, J., and Paschke, R. (2004). Insulin resistance-inducing cytokines differentially regulate SOCS mRNA expression via growth factor- and Jak/Stat-signaling pathways in 3T3-L1 adipocytes. J. Endocrinol. *181*, 129–138.

Fried, S.K., Bunkin, D.A., and Greenberg, A.S.J. (1998). Omental and subcutaneous adipose tissues of obese subjects release interleukin-6: depot difference and regulation by glucocorticoid. J. Clin. Endocrinol. Metab. *83*, 847–850.

Friedman, J.M., and Halaas, J.L. (1998). Leptin and the regulation of body weight in mammals. Nature *395*, 763–770.

Guilherme, A., Virbasius, J.V., Puri, V., and Czech, M.P. (2008). Adipocyte dysfunctions linking obesity to insulin resistance and type 2 diabetes. Nat. Rev. Mol. Cell Biol. *9*, 367–377.

He, Z., and Bateman, A. (2003). Progranulin (granulin-epithelin precursor, PC-cell-derived growth factor, acrogranin) mediates tissue repair and tumorigenesis. J. Mol. Med. *81*, 600–612.

He, Z., Ismail, A., Kriazhev, L., Sadvakassova, G., and Bateman, A. (2002). Progranulin (PC-cell-derived growth factor/acrogranin) regulates invasion and cell survival. Cancer Res. *62*, 5590–5596.

Hotamisligil, G.S. (2006). Inflammation and metabolic disorders. Nature *444*, 860–867.

Hotamisligil, G.S., Murray, D.L., Choy, L.N., and Spiegelman, B.M. (1994). Tumor necrosis factor α inhibits signaling from the insulin receptor. Proc. Natl. Acad. Sci. USA *91*, 4854–4858.

Hotamisligil, G.S., Arner, P., Caro, J.F., Atkinson, R.L., and Spiegelman, B.M. (1995). Increased adipose tissue expression of tumor necrosis factor-α in human obesity and insulin resistance. J. Clin. Invest. *95*, 2409–2415.

Howard, J.K., and Flier, J.S. (2006). Attenuation of leptin and insulin signaling by SOCS proteins. Trends Endocrinol. Metab. *17*, 365–371.

Inoue, H., Ogawa, W., Asakawa, A., Okamoto, Y., Nishizawa, A., Matsumoto, M., Teshigawara, K., Matsuki, Y., Watanabe, E., Hiramatsu, R., et al. (2006). Role of hepatic STAT3 in brain-insulin action on hepatic glucose production. Cell Metab. *3*, 267–275.

Kahn, B.B., and Flier, J.S. (2000). Obesity and insulin resistance. J. Clin. Invest. *106*, 473–481.

Kayasuga, Y., Chiba, S., Suzuki, M., Kikusui, T., Matsuwaki, T., Yamanouchi, K., Kotaki, H., Horai, R., Iwakura, Y., and Nishihara, M. (2007). Alteration of

behavioural phenotype in mice by targeted disruption of the progranulin gene. Behav. Brain Res. *185*, 110–118.

Kern, P.A., Ranganathan, S., Li, C., Wood, L., and Ranganathan, G. (2001). Adipose tissue tumor necrosis factor and interleukin-6 expression in human obesity and insulin resistance. Am. J. Physiol. Endocrinol. Metab. *280*, E745–E751.

Kessenbrock, K., Fröhlich, L., Sixt, M., Lämmermann, T., Pfister, H., Bateman, A., Belaaouaj, A., Ring, J., Ollert, M., Fässler, R., and Jenne, D.E. (2008). Proteinase 3 and neutrophil elastase enhance inflammation in mice by inactivating antiinflammatory progranulin. J. Clin. Invest. *118*, 2438–2447.

Klover, P.J., Zimmers, T.A., Koniaris, L.G., and Mooney, R.A. (2003). Chronic exposure to interleukin-6 causes hepatic insulin resistance in mice. Diabetes *52*, 2784–2789.

Klover, P.J., Clementi, A.H., and Mooney, R.A. (2005). Interleukin-6 depletion selectively improves hepatic insulin action in obesity. Endocrinology *146*, 3417–3427.

Kuyama, H., Watanabe, M., Toda, C., Ando, E., Tanaka, K., and Nishimura, O. (2003). An approach to quantitative proteome analysis by labeling tryptophan residues. Rapid Commun. Mass Spectrom. *17*, 1642–1650.

Lagathu, C., Bastard, J.P., Auclair, M., Maachi, M., Capeau, J., and Caron, M. (2003). Chronic interleukin-6 (IL-6) treatment increased IL-6 secretion and induced insulin resistance in adipocyte: prevention by rosiglitazone. Biochem. Biophys. Res. Commun. *311*, 372–379.

Lago, F., Dieguez, C., Gómez-Reino, J., and Gualillo, O. (2007). Adipokines as emerging mediators of immune response and inflammation. Nat. Clin. Pract. Rheumatol. *3*, 716–724.

Lu, R., and Serrero, G. (2001). Mediation of estrogen mitogenic effect in human breast cancer MCF-7 cells by PC-cell-derived growth factor (PCDGF/granulin precursor). Proc. Natl. Acad. Sci. USA *98*, 142–147.

Matsuo, E., Watanabe, M., Kuyama, H., and Nishimura, O. (2009). A new strategy for protein biomarker discovery utilizing 2-nitrobenzenesulfenyl (NBS) reagent and its applications to clinical samples. J. Chromatogr. B Analyt. Technol. Biomed. Life Sci. *877*, 2607–2614.

Mohamed-Ali, V., Goodrick, S., Rawesh, A., Katz, D.R., Miles, J.M., Yudkin, J.S., Klein, S., and Coppack, S.W. (1997). Subcutaneous adipose tissue releases interleukin-6, but not tumor necrosis factor-α, in vivo. J. Clin. Endocrinol. Metab. *82*, 4196–4200.

Mooney, R.A. (2007). Counterpoint: Interleukin-6 does not have a beneficial role in insulin sensitivity and glucose homeostasis. J. Appl. Physiol. *102*, 816–818, discussion 818–819.

Okamura, N., Masuda, T., Gotoh, A., Shirakawa, T., Terao, S., Kaneko, N., Suganuma, K., Watanabe, M., Matsubara, T., Seto, R., et al. (2008). Quantitative proteomic analysis to discover potential diagnostic markers and therapeutic targets in human renal cell carcinoma. Proteomics *8*, 3194–3203.

Olefsky, J.M. (2000). Treatment of insulin resistance with peroxisome proliferator-activated receptor γ agonists. J. Clin. Invest. *106*, 467–472.

Perkins, D.N., Pappin, D.J., Creasy, D.M., and Cottrell, J.S. (1999). Probability-based protein identification by searching sequence databases using mass spectrometry data. Electrophoresis *20*, 3551–3567.

Pickup, J.C., Mattock, M.B., Chusney, G.D., and Burt, D. (1997). NIDDM as a disease of the innate immune system: association of acute-phase reactants and interleukin-6 with metabolic syndrome X. Diabetologia *40*, 1286–1292.

Qi, D., and Rodrigues, B. (2007). Glucocorticoids produce whole body insulin resistance with changes in cardiac metabolism. Am. J. Physiol. Endocrinol. Metab. *292*, E654–E667.

Rønn, S.G., Billestrup, N., and Mandrup-Poulsen, T. (2007). Diabetes and suppressors of cytokine signaling proteins. Diabetes *56*, 541–548.

Rotter, V., Nagaev, I., and Smith, U. (2003). Interleukin-6 (IL-6) induces insulin resistance in 3T3-L1 adipocytes and is, like IL-8 and tumor necrosis factor-α, overexpressed in human fat cells from insulin-resistant subjects. J. Biol. Chem. *278*, 45777–45784.

Sabio, G., Das, M., Mora, A., Zhang, Z., Jun, J.Y., Ko, H.J., Barrett, T., Kim, J.K., and Davis, R.J. (2008). A stress signaling pathway in adipose tissue regulates hepatic insulin resistance. Science *322*, 1539–1543.

Sachithanandan, N., Fam, B.C., Fynch, S., Dzamko, N., Watt, M.J., Wormald, S., Honeyman, J., Galic, S., Proietto, J., Andrikopoulos, S., et al. (2010). Liver-specific suppressor of cytokine signaling-3 deletion in mice enhances hepatic insulin sensitivity and lipogenesis resulting in fatty liver and obesity. Hepatology *52*, 1632–1642.

Sakoda, H., Ogihara, T., Anai, M., Funaki, M., Inukai, K., Katagiri, H., Fukushima, Y., Onishi, Y., Ono, H., Fujishiro, M., et al. (2000). Dexamethasone-induced insulin resistance in 3T3-L1 adipocytes is due to inhibition of glucose transport rather than insulin signal transduction. Diabetes *49*, 1700–1708.

Satoh-Horikawa, K., Nakanishi, H., Takahashi, K., Miyahara, M., Nishimura, M., Tachibana, K., Mizoguchi, A., and Takai, Y. (2000). Nectin-3, a new member of immunoglobulin-like cell adhesion molecules that shows homophilic and heterophilic cell-cell adhesion activities. J. Biol. Chem. *275*, 10291–10299.

Senn, J.J., Klover, P.J., Nowak, I.A., and Mooney, R.A. (2002). Interleukin-6 induces cellular insulin resistance in hepatocytes. Diabetes *51*, 3391–3399.

Senn, J.J., Klover, P.J., Nowak, I.A., Zimmers, T.A., Koniaris, L.G., Furlanetto, R.W., and Mooney, R.A. (2003). Suppressor of cytokine signaling-3 (SOCS-3), a potential mediator of interleukin-6-dependent insulin resistance in hepatocytes. J. Biol. Chem. *278*, 13740–13746.

Shi, H., Tzameli, I., Bjørbaek, C., and Flier. (2004). Suppressor of cytokine signaling 3 is a physiological regulator of adipocyte insulin signaling. J. Biol. Chem. *279*, 34733–34740.

Shoelson, S.E., Herrero, L., and Naaz, A. (2007). Obesity, inflammation, and insulin resistance. Gastroenterology *132*, 2169–2180.

Tang, W., Lu, Y., Tian, Q.Y., Zhang, Y., Guo, F.J., Liu, G.Y., Syed, N.M., Lai, Y., Lin, E.A., Kong, L., et al. (2011). The growth factor progranulin binds to TNF receptors and is therapeutic against inflammatory arthritis in mice. Science *332*, 478–484.

Torisu, T., Sato, N., Yoshiga, D., Kobayashi, T., Yoshioka, T., Mori, H., Iida, M., and Yoshimura, A. (2007). The dual function of hepatic SOCS3 in insulin resistance in vivo. Genes Cells *12*, 143–154.

Turnbow, M.A., Keller, S.R., Rice, K.M., and Garner, C.W. (1994). Dexamethasone down-regulation of insulin receptor substrate-1 in 3T3-L1 adipocytes. J. Biol. Chem. *269*, 2516–2520.

Ueki, K., Kondo, T., and Kahn, C.R. (2004). Suppressor of cytokine signaling 1 (SOCS-1) and SOCS-3 cause insulin resistance through inhibition of tyrosine phosphorylation of insulin receptor substrate proteins by discrete mechanisms. Mol. Cell. Biol. *24*, 5434–5446.

Uysal, K.T., Wiesbrock, S.M., Marino, M.W., and Hotamisligil, G.S. (1997). Protection from obesity-induced insulin resistance in mice lacking TNF-α function. Nature *389*, 610–614.

van Putten, J.P., Wieringa, T., and Krans, H.M. (1985). Corticosteroids as long-term regulators of the insulin effectiveness in mouse 3T3 adipocytes. Diabetologia *28*, 445–451.

Waki, H., and Tontonoz, P. (2007). Endocrine functions of adipose tissue. Annu. Rev. Pathol. *2*, 31–56.

Wallenius, V., Wallenius, K., Ahrén, B., Rudling, M., Carlsten, H., Dickson, S.L., Ohlsson, C., and Jansson, J.O. (2002). Interleukin-6-deficient mice develop mature-onset obesity. Nat. Med. *8*, 75–79.

Watanabe, M., Takemasa, I., Kawaguchi, N., Miyake, M., Nishimura, N., Matsubara, T., Matsuo, E., Sekimoto, M., Nagai, K., Matsuura, N., et al. (2008). An application of the 2-nitrobenzenesulfenyl method to proteomic profiling of human colorectal carcinoma: A novel approach for biomarker discovery. Proteomics Clin Appl *2*, 925–935.

Weisberg, S.P., McCann, D., Desai, M., Rosenbaum, M., Leibel, R.L., and Ferrante, A.W., Jr. (2003). Obesity is associated with macrophage accumulation in adipose tissue. J. Clin. Invest. *112*, 1796–1808.

Wellen, K.E., and Hotamisligil, G.S. (2005). Inflammation, stress, and diabetes. J. Clin. Invest. *5*, 1111–1119.

Xu, H., Barnes, G.T., Yang, Q., Tan, G., Yang, D., Chou, C.J., Sole, J., Nichols, A., Ross, J.S., Tartaglia, L.A., and Chen, H. (2003). Chronic inflammation in fat plays a crucial role in the development of obesity-related insulin resistance. J. Clin. Invest. *112*, 1821–1830.

Youn, B.S., Bang, S.I., Klöting, N., Park, J.W., Lee, N., Oh, J.E., Pi, K.B., Lee, T.H., Ruschke, K., Fasshauer, M., et al. (2009). Serum progranulin concentrations may be associated with macrophage infiltration into omental adipose tissue. Diabetes *58*, 627–636.

Zanocco-Marani, T., Bateman, A., Romano, G., Valentinis, B., He, Z.H., and Baserga, R. (1999). Biological activities and signaling pathways of the granulin/epithelin precursor. Cancer Res. *59*, 5331–5340.

Zhu, J., Nathan, C., Jin, W., Sim, D., Ashcroft, G.S., Wahl, S.M., Lacomis, L., Erdjument-Bromage, H., Tempst, P., Wright, C.D., and Ding, A. (2002). Conversion of proepithelin to epithelins: roles of SLPI and elastase in host defense and wound repair. Cell *111*, 867–878.